Evaluation of Seismic Hazard and Site Geodynamic Properties by Using Geophysical Methods in the North of Iran

Ehsan Pegah[1], Mohsen Mahmoodi[2], Arzhang Siavashpoo[3]
1. School of Civil Engineering and Mechanics, Huazhong University of Science and Technology, Wuhan, China
2. School of Mining, Petroleum and Geophysics Engineering, University of Shahrood, Shahrood, Iran
3. Department of Geophysics, Science and Research Branch of Islamic Azad University, Tehran, Iran
E-mail: epegah@hust.edu.cn

Abstract: In this study two powerful geophysical methods are used in order to evaluate the properties of shallow soil deposits at a specific area for planned power plants construction purposes. Twenty five seismic refraction survey lines were conducted at the study area to record the vertical movements of the ground. The acquired shot gathers were processed and then the information of primary wave (P-wave) and shear wave (S-wave) velocities derived. The P-wave velocities were obtained by using the Seismic Refraction Tomography method (SRT) while the S-wave velocities were extracted by utilizing the Multichannel Analysis of Surface Waves (MASW) technique, which is established based on Rayleigh waves dispersion characteristics. The resulted wave velocities information used to predict the seismic hazard level and dynamic behavior of the soil and bedrock layers. By this information the assessment of site characterization was carried out. The obtained results show that the western central and southern central parts of the area are characterized by less competent soil layer quality whereas elsewhere are specified by more competent soil deposits and less hazard risk for any engineering purposes.
Keywords: Seismic Refraction Tomography, Multichannel Analysis of Surface Waves, wave velocity, soil, bedrock, geotechnical site characterization.

1. Introduction

Geophysical tests based on the generation and propagation of seismic waves are widely used in earthquake geotechnical engineering. Seismic in-situ tests are often the only way to determine soil stiffness in undisturbed conditions, especially for coarse grain soils, in which undisturbed sampling is problematic. In this regard, seismic refraction surveying as one of the main and cost-effective geophysical methods can be used to investigate the near-surface structures, layering, local anomalies and etc.

Conventional interpretation of seismic refraction data visualize the subsurface as a layered medium where each layer has a discrete seismic velocity. With this assumption and measuring the travel times of refracted seismic waves, the thickness and dip angle of each layer can be achieved [21]. Nowadays, interpretation methods are being developed and refraction tomography is one of the main techniques to constrain the three-dimensional (3D) distribution of physical properties that affect the seismic waves propagation [24]. It makes the possibility to model velocity variations as a continuous gradient across a grid or mesh under the seismic profiles. This method is a type of inverse problem which use the ray tracing algorithm to determine gradual velocity variations and exactly considers the ray paths for the first arrival waves that pass through the ground interior. Several recent studies of [20], [5], [3], [4] and [6] prove the high ability of SRT technique in the subsurface velocities modeling and extracting the desired information. They indicated that refraction tomography performs well in many situations where traditional refraction techniques fail in identifying both vertical and horizontal velocity gradients.

The average P-wave velocity can be calculated by using the seismic refraction tomography (SRT) method. Forward modeling methods can be employed and the ray tracing between source locations and receivers can be carried out iteratively in the initial assumed model. The algorithm compares the calculated traveltime with the observed traveltime to modify the model. This process will be repeated over and over until the Root-Mean-Square (RMS) error between the observed and calculated traveltime become minimized. One of the most important advantages of this algorithm is that it makes no assumption on the direction of subsurface velocity gradient ([3] and [4]). Therefore, it can detect the velocity variations in both vertical and horizontal directions

accurately. Eventually, the final resulted section shows the velocity gradient along the seismic profile versus the depth for the subsurface area.

One of the most recent techniques for shear wave (S-wave) velocity estimation in soil profile is using the characteristics of Rayleigh wave dispersion. Although other direct methods, such as up-hole, down-hole and cross-hole surveys can be used, they are generally more expensive than the surface wave methods and in areas with technical constraints can't be performed. Rayleigh wave is one kind of surface waves that is always generated in all seismic surveys. It has the strongest energy with the highest signal- to-noise ratio (S/N). Rayleigh waves are consisted of a frequency range that each frequency component travels by an individual velocity with the name of phase velocity. This phenomenon is called dispersion, which introduces Rayleigh waves as dispersive waves. The penetration depth of each component depends on its wavelength and the propagation velocity is directly related to the S-wave velocity of medium. The multichannel analysis of surface waves (MASW) is an efficient technique that utilizes these properties to extract the S-wave velocity profile along the soil column. The main advantage of this method is its ability to take full account of the complicated nature of seismic waves that always contain distracting noises [17]. This method was successfully used and recommended as a satisfactory technique in studies of many researchers ([27], [28], [16], [25], [17], [14], [2], [26], [19], [23], [15], [22] and [1]).

In this study, non-invasive seismic refraction profiles are conducted, processed and analyzed to evaluate the geotechnical features in the site of Siahpoush power plants in Iran. The P-wave and S-wave velocities were firstly obtained by SRT and MASW methods respectively for the seismic refraction profiles in the study area. These two sets of velocities were then employed to evaluate the dynamic properties and seismic hazard levels to recommend the most suitable zone for construction purposes.

2. Geographical location and Geology of the area

The study area is being planned and designed for the construction of a wind farm and the associated power plants. The study area (Fig. 1) covers an area of 8.2 km2 and is located between longitude 49º 17′ 25.51″ E and 49º 19′ 03.09″ E, and latitude 36º 43′ 30.32″ N and 36º 41′ 39.30″ N. It lies about 10 km to the west side of Manjil City in northern Iran. This area is bounded by the Sefid-Rud Lake in the north and the Siahpoush village in the south side. The general topography of the study area includes smooth plain in the east that changes to foothills while moving to the west.

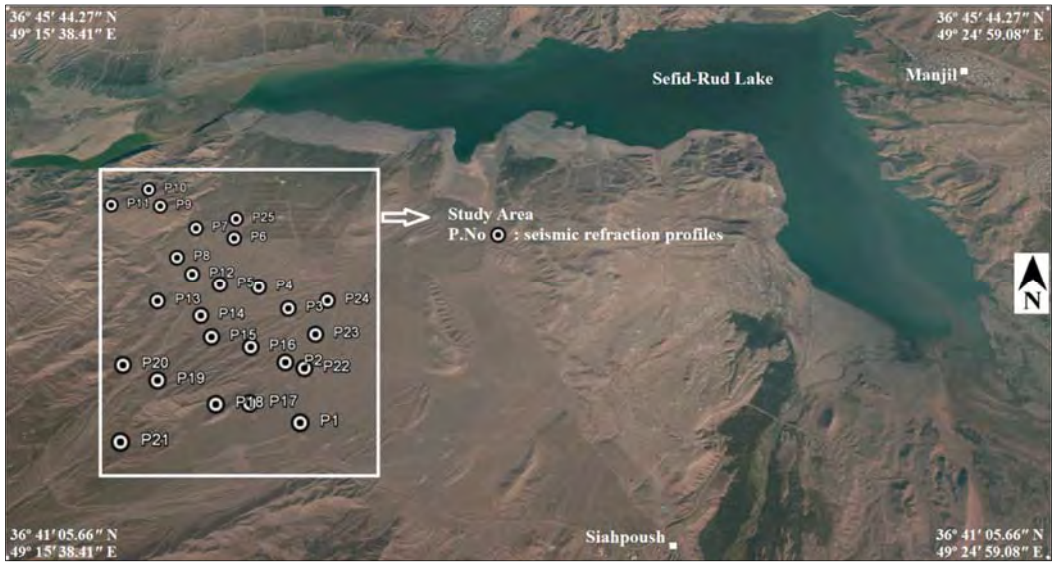

Fig. 1 Geographical Location map of the study area and the seismic refraction profiles.

This area contains soils and rocks that are related to the Cenozoic era. The whole study area is covered by recent alluvium where according to surficial geological information and some drilled boreholes, the shallow materials mostly consist of a mixture of sand and gravel. Below the deposits, sandstones, conglomerates rock layers and andesitic tuffs can be found. The geology periods of the soil deposits and the rock formations are referred to as the Quaternary (Holocene epoch) and Neogene to Quaternary (Pliocene and Pleistocene epochs), respectively.

3. Seismic Data Acquisition

In this study our main objectives are to estimate the P-wave and S-wave velocity of shallow layers to determine their geotechnical features. In order to increase the penetration depth, the frequency content of the recorded Rayleigh waves should be low enough to result longer wavelengths. Hence, we accomplished an optimum seismic refraction survey which recorded the desired frequency range and penetration depth. P-waves and Rayleigh-waves were collected at various sites where windy turbines and power plants have been planned. Twenty five linear seismic refraction profiles were conducted to cover the study area (Fig 1). Table 1 summarized the seismic acquisition parameters in this survey. Different kinds of seismic waves in a wide range of frequencies were acquired by the incident energy generated by each seismic source. Some ambient noises such as daily human activities, river water flow, equipment activities from nearby structures and wind noises were serious difficulties in the field. Those caused decreasing signal to noise ratio (S/N) in some parts of shot gathers. Some processing techniques were employed to enhance this ratio to desired values. Fig. 2 shows a recorded raw shot gather at the left end and its Amplitude-Frequency spectrum at profile No.9.

Table 1 Seismic acquisition parameters in the study area.

Parameter	**setting**
Spread configuration	Linear
Spread length	69 m
Total number of geophones	24 (for each profile)
Geophone interval	3 m
Geophone type	4.5 Hz vertical component
Total number of shots	3 (for each profile)
Shot locations	Two source points were located 25 m away from the two ends of the geophone array and the third one was located in the middle of the spread.
Source equipment	Sledgehammer (8kg) and Steel plate (20 cm×20 cm×5 cm).
Stacking number	10 to 15
Sampling interval	0.5 millisecond (ms)
Record length	1024 millisecond (ms)
Total number of samples	2048 per trace
Seismograph recording System	ABEM Terraloc MK8

4. Seismic Data Processing

4.1. S-waves

In MASW method dispersion curve of Rayleigh waves can be calculated by applying Fourier transform in both time and space on the field data and then selecting the maximum values of energy density (the highest amplitudes) in this domain. The original waves field is converted into an image of the energy density as a function of the frequency and of the wavenumber (*f-k* spectrum) by application of the 2D Fourier transform (Eq. 1).

$$\bar{u}(f,k) = \sum_{l=0}^{M-1}\left[\sum_{m=0}^{N-1} u_{l,m}.\, e^{-i\left(f\frac{2\pi}{N}m\right)}\right].\, e^{-i\left(k\frac{2\pi}{N}l\right)} \quad (1)$$

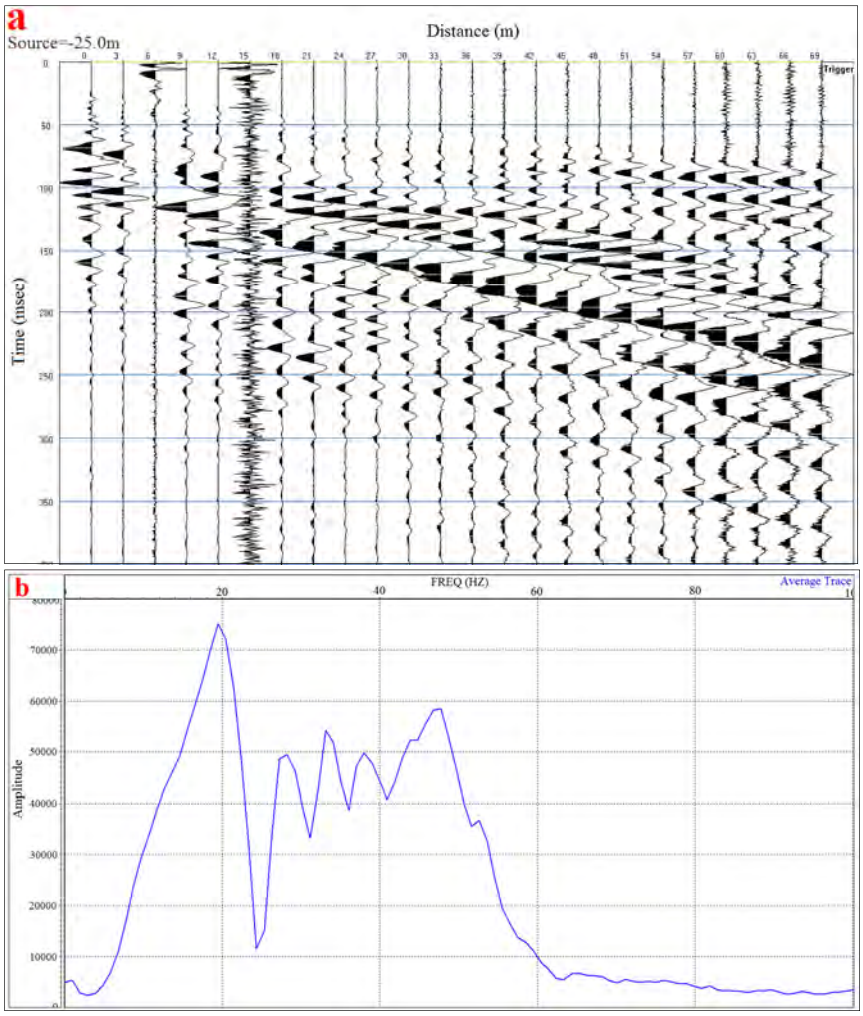

Fig. 2 (a) The left side recorded raw shot gather of Profile No. 9, and (b) its average Amplitude-Frequency spectrum.

Where N is the number of samples that are taken along a trace, M is the number of receivers along a straight line in field data acquisition, f is the frequency, k is the wavenumber, m is the index of samples and l is the index of receivers.

In this domain, there are some points with associated coordinates of (f_{max}, k_{max}), which have the maximum energies. They can be used to evaluate the dispersion curve since phase velocity is given by the ratio between frequency and wavenumber. Phase velocity of Rayleigh wave (V_R) and associated dispersion curve can be chosen by picking the spectral maxima:

$$V_R = \frac{2\pi f_{max}}{k_{max}} \tag{2}$$

At last, an initial theoretical dispersion curve (initial model of shear wave velocity versus depth) is assumed and by iterating the inversion process was repeated until acceptable accuracy is achieved. Once the inversion is completed, the final model of S-wave velocity versus depth can be achieved.

In this study, the MASW data processing was carried out by using the SeisImager/SW software version 3.14 and VISTA 2D/3D Seismic Data Processing version 10.0 through spectral inversion to determine the S-wave profiles in the area. Since extracting accurate shear wave velocity profile depends on the generation of high quality dispersion curve, after geometry assignment some processing steps including denoising and true amplitude recovery on the shot gathers was carried out. Fig. 3 shows the shot gather of Fig. 2a and its Amplitude-Frequency spectrum after this process. The processed shot gather was converted through 2D transformation, resulting in the dispersion image panel in a specified frequency range (Fig. 4a). The desired dispersion curve of the fundamental mode of the Rayleigh wave was then extracted by picking the highest energy accumulation pattern of this image panel (Fig. 4b). Each dispersion curve was individually inverted to

generate a 1D (depth) shear wave velocity profile. The inversion program iteratively modified the initial model to minimize its difference with the observed data. The RMS error should be less than 5%. 1D S-wave velocity profiles were finally obtained. These 1D profiles were assigned to the middle point of the geophone spreads and were the best representation of the subsurface materials specifications. Average velocity in a layered soil column with thicknesses d_1, d_2, …, d_n and interval velocities V_{s1}, V_{s2}, …, V_{sn} can be calculated by Eq. (3):

$$V_{s(ave)} = \frac{\sum_{i=1}^{n} d_i}{\sum_{i=1}^{n} \frac{d_i}{V_{si}}} \tag{3}$$

Fig. 5 illustrates the 1D S-wave velocity profile at the seismic profile No. 9 deduced from the inversion technique.

4.2. P-waves

Based on seismic refraction tomography, the collected P-waves data for each seismic line were processed and analyzed using commercial SeisImager/2D software package version 3.14 and VISTA 2D/3D Seismic Data Processing version 10.0. At first, the raw field data were read and the geometry assignment was given. The wave forms were analyzed by first arrival picking, the traveltime-distance curves were determined, and finally the average P-wave velocities in the soil layers and bedrocks were achieved for each profile.

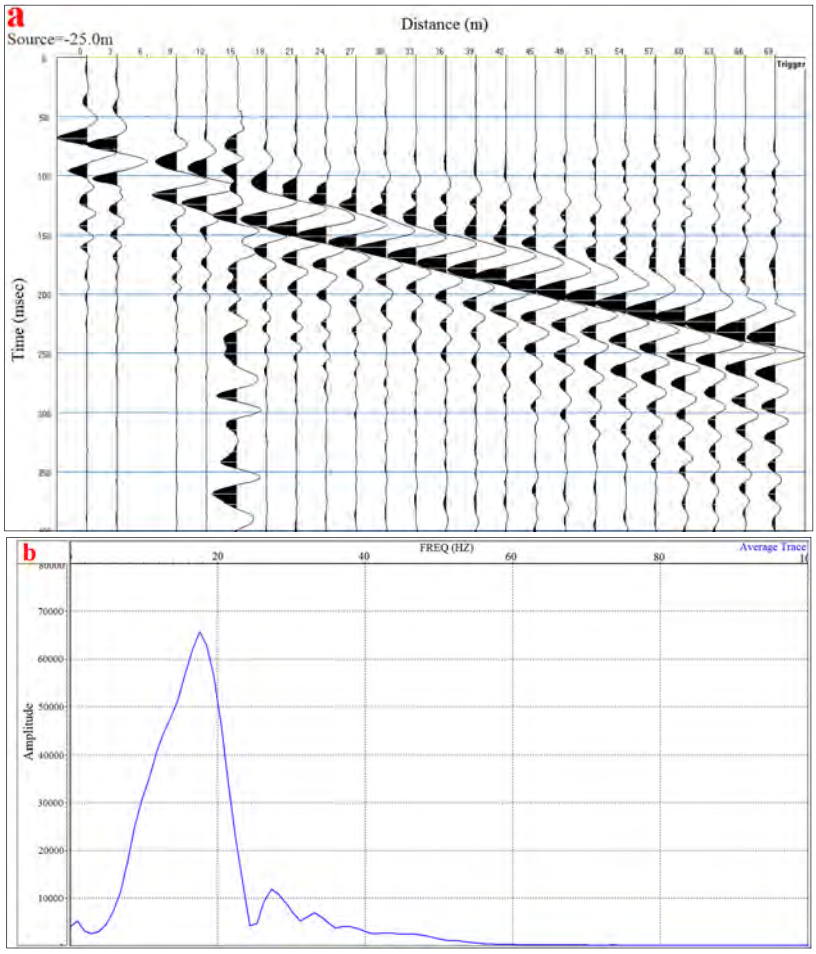

Fig. 3 (a) The left side recorded raw shot gather of Profile No. 9 after applying the processing sequence, and (b) its average Amplitude-Frequency spectrum.

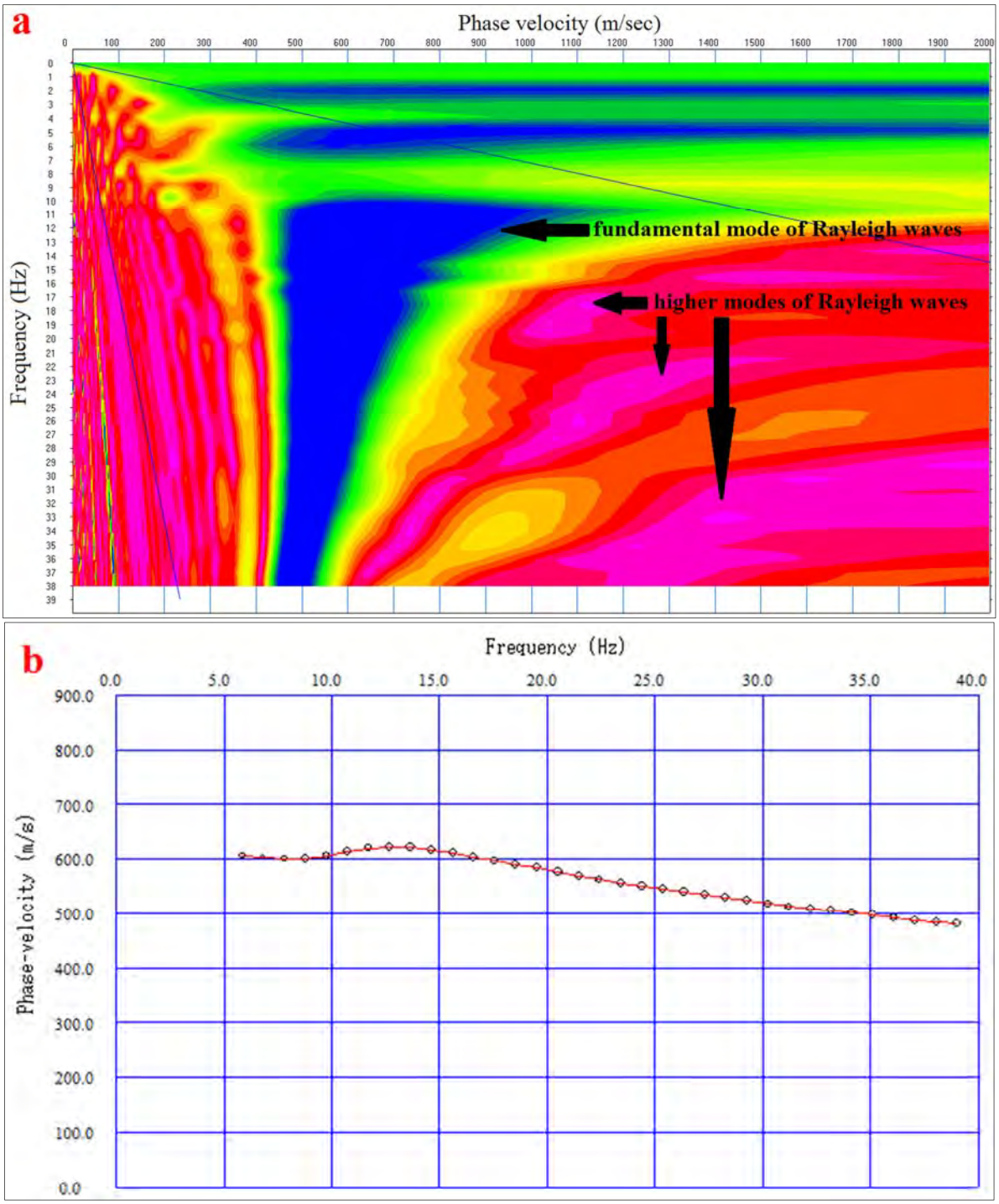

Fig. 4 (a) The dispersion image and (b) the dispersion curve (phase velocity versus frequency) deduced from the recorded surface waves at profile No. 9.

5. Results and discussion

5.1. P-wave and S-wave velocities

It is observed that overall the S-wave velocity increased with depth and at a special depth it was greater than 760 m/s. According to NEHRP ([8]), when the shear wave velocity in a subsurface layer reaches this value (V_s > 760 m/s), that layer can be classified as bedrock, while the materials having smaller velocities and laying over the bedrock are the soil deposits. Fig. 6a illustrates the 2D map of the bedrock depth (or soil thickness) distribution at the study area. As can be seen, the southern parts of the area were characterized by smaller soil thickness and the least thickness was 13 m. The soil thickness increases towards the eastern side, where its value was larger than 40 m. The variations of the P-wave and S-wave velocities of the bedrock were small in the area,

ranging from 1300 (Profile 1) to 1540 m/s (Profile 18) for the P-wave and 760 (Profile 6) to 850 m/s (Profile 23) for the S-wave, respectively, as shown in Fig. 6b and Fig. 6c. The obtained average S-wave and P-wave velocities of the soil layer were also mapped, the results of which are shown in Figs. 7a and 7b. The average P-wave velocities of the soil layer varied between 510 (Profile 19) and 920 m/s (Profile 18), while the average S-wave velocities ranged from 289 (Profile 19) to 576 m/s (Profile 18) in the area. The distributions of the P-wave and S-wave velocities are similar, and they indicated the existence of soft soil deposits in the western and southern central parts.

5.2. Geotechnical site characterization

The study area is located in a high seismic hazard zone. One of the largest earthquakes in Iran occurred close to the study area in 1990 with a moment magnitude of 7.4, and the structural design of the planned wind farm and power plants shall consider seismic loading. The shear wave velocity is the best indicator of the ground stiffness and is also considered as a key factor for the seismic site response of the ground. Characteristics of strong ground motions, such as amplitudes and frequencies, are modified by the soil layers, which are directly determined by the average shear wave velocity at a site. In many cases, the damages caused by earthquakes have been the consequence of the interaction between strong ground motion and soil stiffness, or the so-called “site effect”. An accurate estimation of the site effects is therefore a major challenge for an efficient mitigation of the seismic risk. In the following, seismic site characterization of the study area will be discussed.

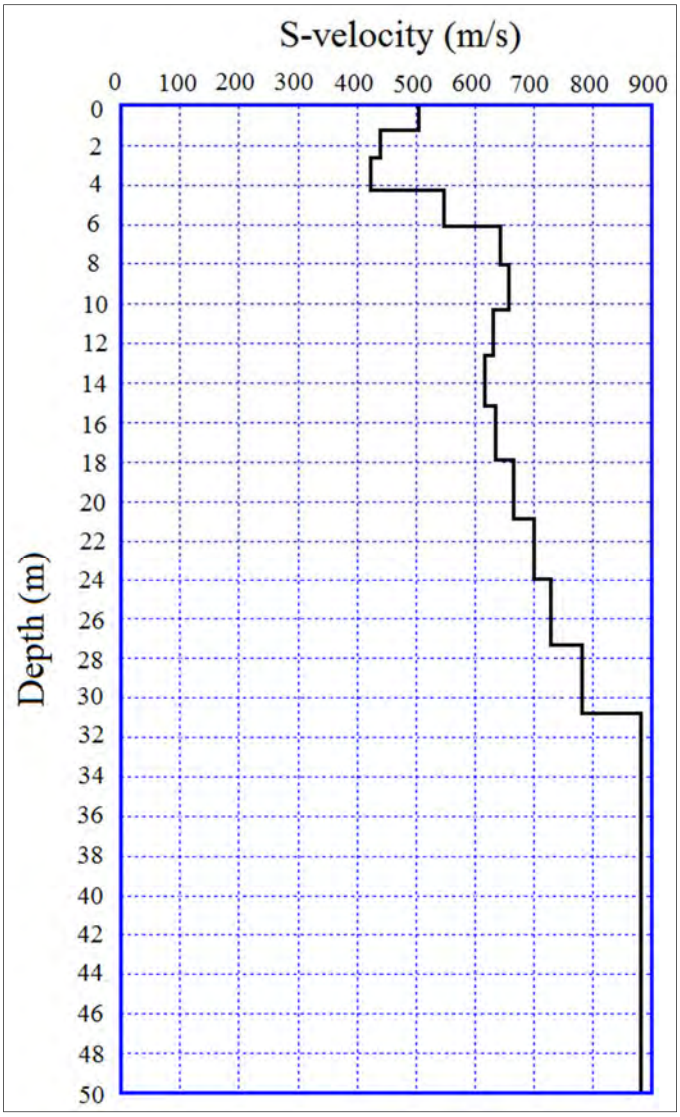

Fig. 5 1D S-wave velocity profile at location No. 9 deduced from the inversion technique.

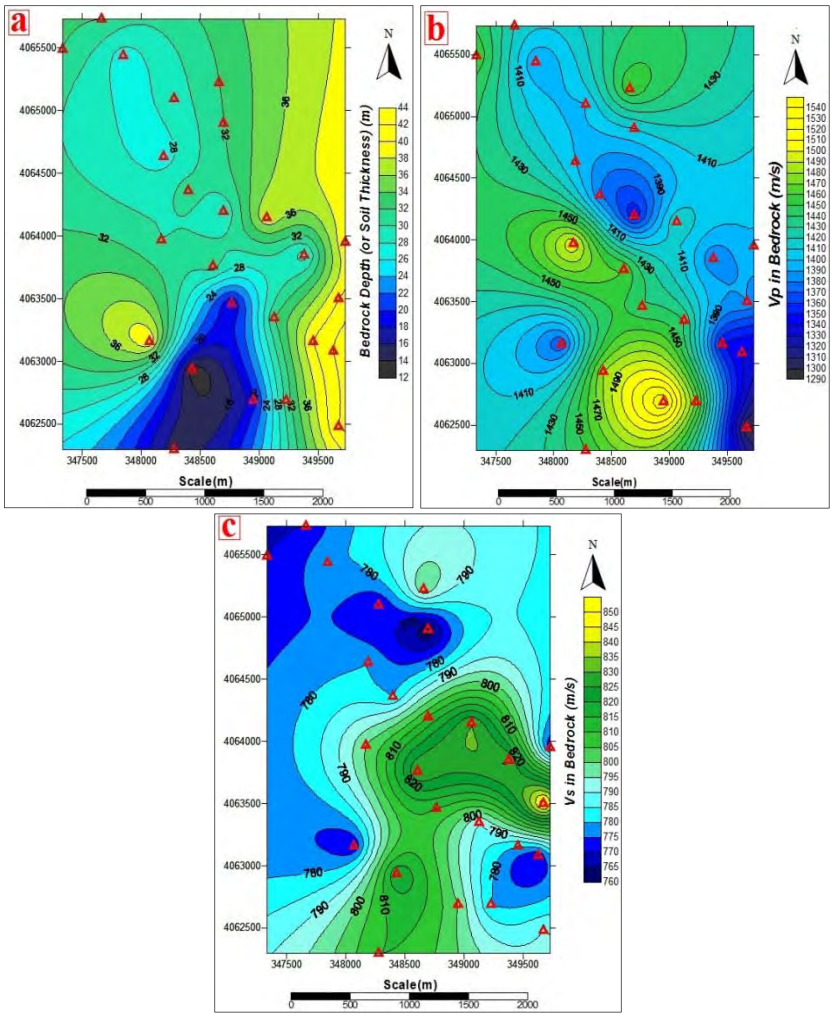

Fig. 6 (a) The bedrock depth (or soil thickness) distribution contour map in the study area. (b) P-wave velocity distribution contour map of the bedrock resulted from SRT method. (c) S-wave velocity distribution contour map of the bedrock resulted from MASW method.

5.2.1. Fundamental site periods

The site periods for shallow and deep soil deposits are different and depend on some parameters. For a soil column with thickness *H*, the vibration period for a given mode is expressed as following equation ([9]):

$$T_n = \frac{4H}{(2n-1)V_{S(ave)}} \tag{4}$$

Here, *n* represents the harmonic modes and is an integer (1, 2, 3 …) and $V_{s(ave)}$ is the average shear wave velocity in the layer. With *n=1*, the fundamental period of the site will be resulted. The fundamental vibration period of the ground is one of the important parameters that is used to determine regional earthquake risk. In addition, the information of this map is used widely in the seismic soil- structure interaction analyses.

The fundamental vibration period of the soil deposits in the study area were determined and mapped, as shown in Fig. 8. It shows that the minimum value of the fundamental period was 0.11 second (Profile 21) and the maximum value was 0.43 second (Profile 20) for all the 25 different locations. The higher periods (lower resonant frequencies) are concentrated mainly at the western central part while the lower periods (higher resonant frequencies) concentrated at the southern part of the area.

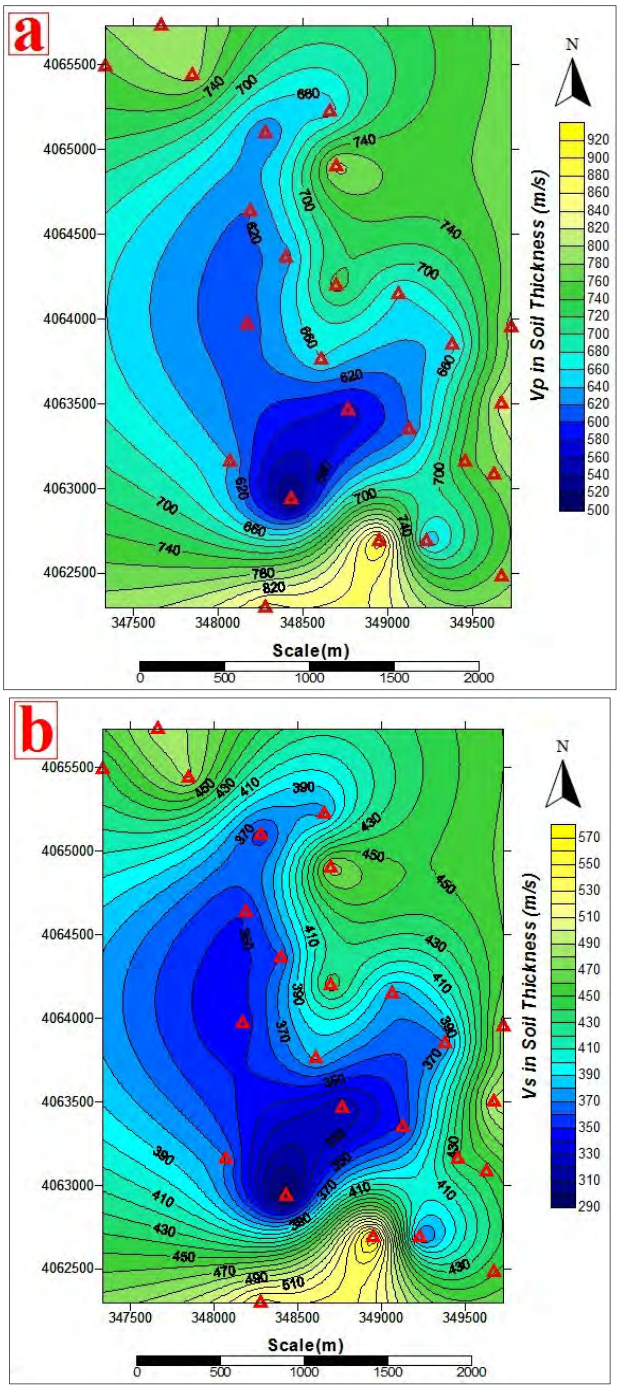

Fig. 7 (a) P-wave velocity distribution contour map in the soil layer resulted from SRT method. (b) S-wave velocity distribution contour map in the soil layer resulted from MASW method.

5.2.2. Site amplification ratios

In a soil medium where velocity is represented by a function of depth, the amplification ratio at an interval equal to a quarter of wavelength down from the surface can be calculated by Eq. (5) ([11]):

$$A = (\rho_r V_{s(r)}/\rho_s V_{s(s)})^{0.5} (\cos i_r/\cos i_s)^{0.5} \quad (5)$$

Where $V_{s(r)}$ and $V_{s(s)}$ are the near-surface velocities of S-wave in rock and soil respectively, ρ_r and ρ_s are the densities and i_r and i_s are the angles of incidence. The factor involving the angles of incidence can be neglected in cases where the angle of incidence in rock is not large. Since, the variation of density versus depth is relatively smaller than the rate of S-wave velocity's variation; therefore the shear wave velocity is the decisive factor in the determination of amplification ratio of the study area.

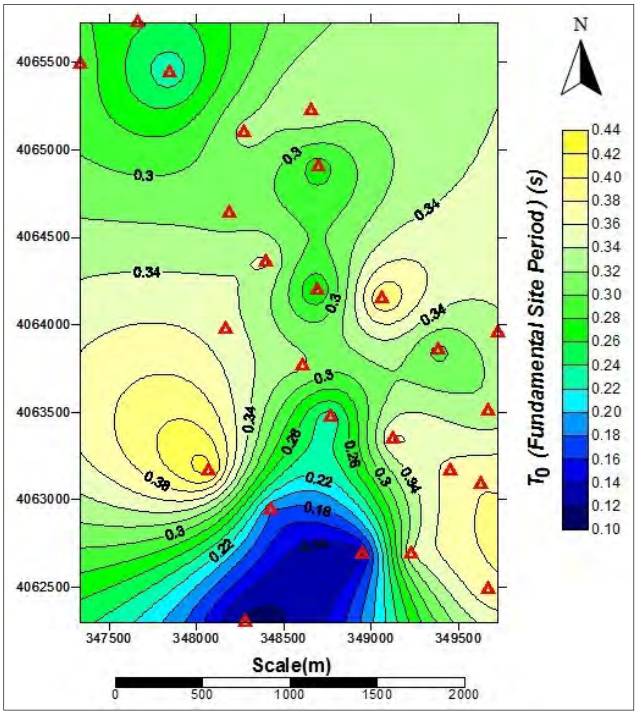

Fig. 8 The fundamental vibration period map of the situated soil deposits over the bedrock surface in the study area.

The density ρ in soil and bedrock layers was calculated by Eq. (6), which is an empirical relation proposed by Gardner et al. ([10]):

$$\rho = 0.31\, V_p^{0.25} \tag{6}$$

Where ρ is in (tm^{-3}) and V_p is in (m/s). In-situ soil density tests at limited locations were also carried out and it was found that the obtained values were close to those predicted by Eq. (6). Amplification ratios of site for angles close to the vertical incidence and frequencies close to 1.5 Hz were calculated. Fig. 9 illustrates amplification ratios distribution in the study area. The amplification factor in the area varies between 1.26 and 1.92. As can be seen, the southern, eastern and northern west regions have been specified by smaller values; while, southern central part has larger values. It is clear that this zone can experience serious damage when occurring considerable earthquakes, while else regions can have moderate to low damages.

5.2.3. Dynamic soil properties of site

The engineering problems governed by wave propagation effects induce low levels of strain in the soil mass. The geophysical field tests as in-situ tests have the advantage that the state of stress is inherently included in the procedure. Additionally, what is tested is a volume of the situated materials under the ground surface between the source and receiver. Geophysical tests propagate the seismic waves through the soil at a very low strain level (less than 10^{-3} percent). This level of strain allows using the elasticity theory for measuring the dynamic properties of soil deposits in the study area. Elastic moduli of Poisson's ratio (ν), Young' modulus (E), shear modulus (G) and Bulk modulus (K) can be obtained using the P-wave and S-wave velocities, as shown in Table 2. The figures of 10, 11, 12 and 13 display the distribution of average values of ν, E, G and K in the soil and bedrock layers of the study area respectively.

ν in soil varies between 0.178 and 0.267 in the study area. Fig. 10a shows that mostly western and central regions of study area are characterized by higher values of ν comparing with other parts. The lower values of ν indicate a relatively more competent soil deposits for any construction project (Table 3). Regarding the achieved values, the soil layer of the study area is classified as competent materials. Figure 10b illustrates that ν in the bedrock is ranging from 0.201 and 0.315 that is a larger variation range in comparison with the soil layer. These values reveal that the bedrock can be classified as moderately competent to competent materials in everywhere of the study area.

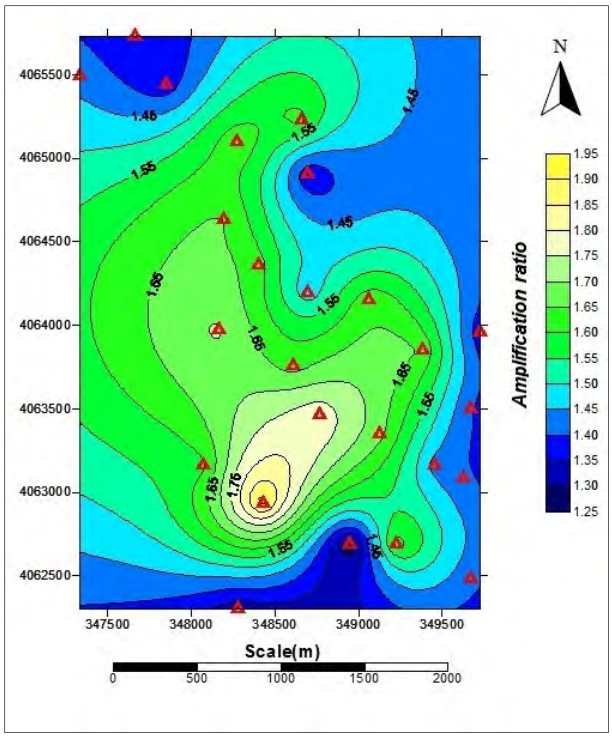

Fig. 9 ¼ wavelength amplification ratios for approximated vertical incidence angles, and frequencies close to 1.5 Hz.

Variation range of E in the soil layer is from 311 to 1334 MPa. Distribution map of E in soil layer (Fig 11a) shows that the southern central and the western parts are specified by lower values while other parts are specified by higher values. E in the bedrock varies between 2788 and 3330 MPa throughout the study area (Fig 11b) which proves the presence of high resistance against the vertical deformations.

G in the soil layer of the study area varies between 123 and 566 MPa. Its distribution contour map (Fig 12a) indicates the soil layer of the southern central and the western regiones have lower resistance against the shear stresses. As can be seen from Fig 12b, this modulus for bedrock is ranging from 1097 to 1368 MPa that displays existence of higher shear strength in this layer.

Variation range of K in soil layer of the study area is from 219 to 690 MPa. Fig. 13a shows distribution contour map this parameter in the soil layer. Bulk modulus in bedrock varies between 1597 and 2948 MPa. Fig. 13b illustrates that except of a narrow band where is mainly concentrated in the lower part of east side of study area, the other places are specified by medium and higher values.

Table 2 Equations for calculating the elastic moduli ([12]).

Elastic Modulus	Equations
Poisson's ratio	$\nu = \frac{1}{2}[1 - \frac{1}{\left(\frac{Vp}{Vs}\right)^2 - 1}]$
Young' modulus	$\mathrm{E} = \rho \frac{3Vp^2 - 4Vs^2}{(Vp/Vs)^2 - 1}$
Shear modulus	$\mathrm{G} = \frac{E}{2(1+\sigma)}$
Bulk modulus	$\mathrm{K} = \frac{E}{3(1-2\sigma)}$

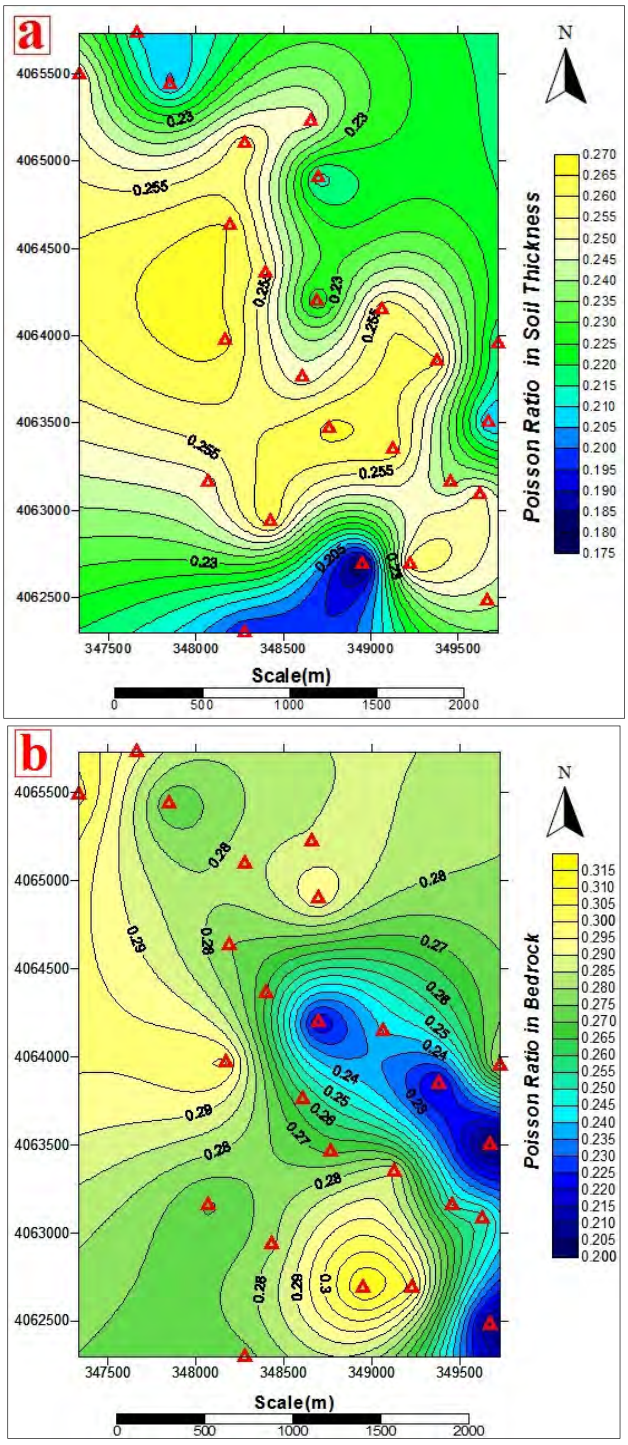

Fig. 10 Poisson's ratio (ν) distribution contour map in the study area. (a) soil layer and (b) bedrock layer.

5.2.4. Results

On the whole, the soil deposits over the bedrock of the study area can be divided into two main zones according to the P-wave and S-wave seismic velocities, elastic moduli and seismicity hazards. The first zone mainly includes the western central and southern central parts where characterized by less competent soils quality. This zone has been characterized by P and S-wave velocities ranging from 510 to 640 m/s and 290 to 360 m/s respectively. The amplification ratio in this zone varies between 1.65 and 1.92 which warns about significant damages when occurring earthquakes with remarkable magnitudes. ν is greater than 0.260 and E, G and K are less than 500 MPa, 200 Mpa and 340 MPa respectively. The second zone mainly includes the northern, eastern and southern parts where the subsurface soil deposits are characterized by more competent soils quality. The P-wave velocity in this zone varies in the range of 640 to 920 m/s while the S-wave velocity is

ranging from 360 to 576 m/s. The variation range of amplification factor is from 1.26 to 1.65 where characterized this zone with lower vulnerability. Poisson's ratio in this zone is less than 0.260 whereas E, G and K are greater than 500 MPa, 200 MPa and 340 MPa respectively. Table 4 indicates a summary of the calculated parameters for the second zone in the study area.

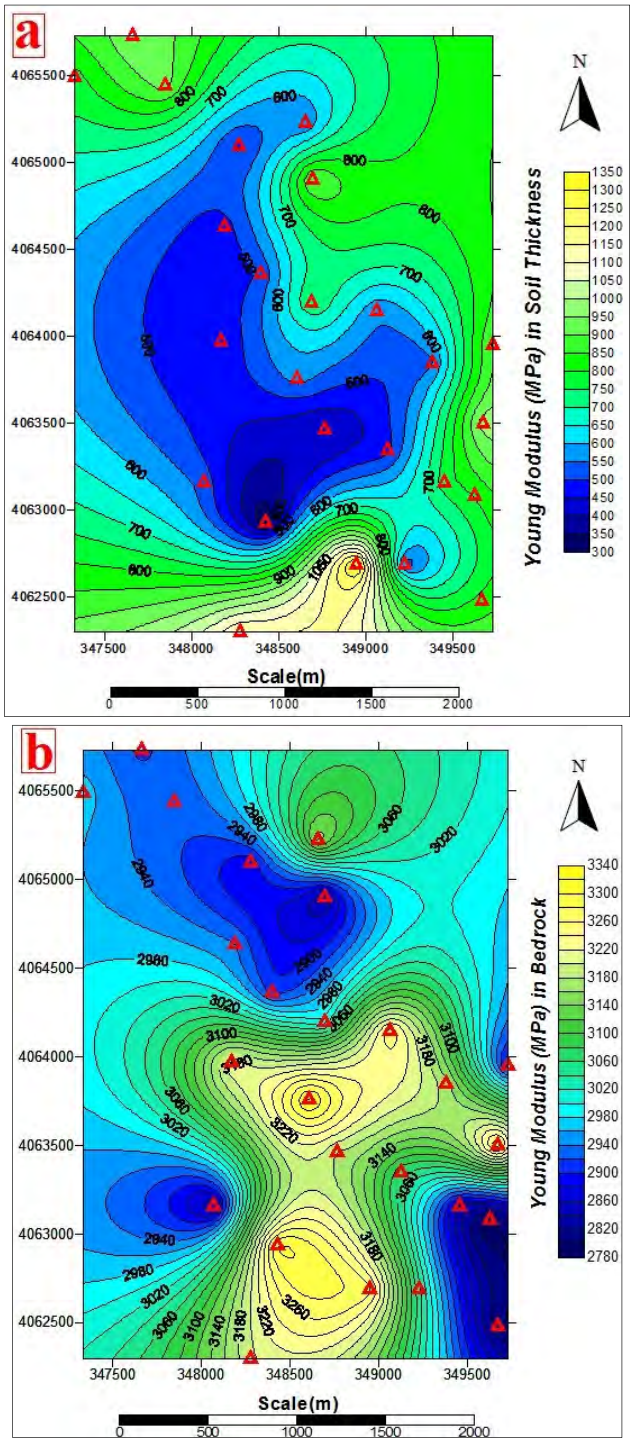

Fig. 11 Young's modulus (E) distribution contour map in the study area. (a) soil layer and (b) bedrock layer.

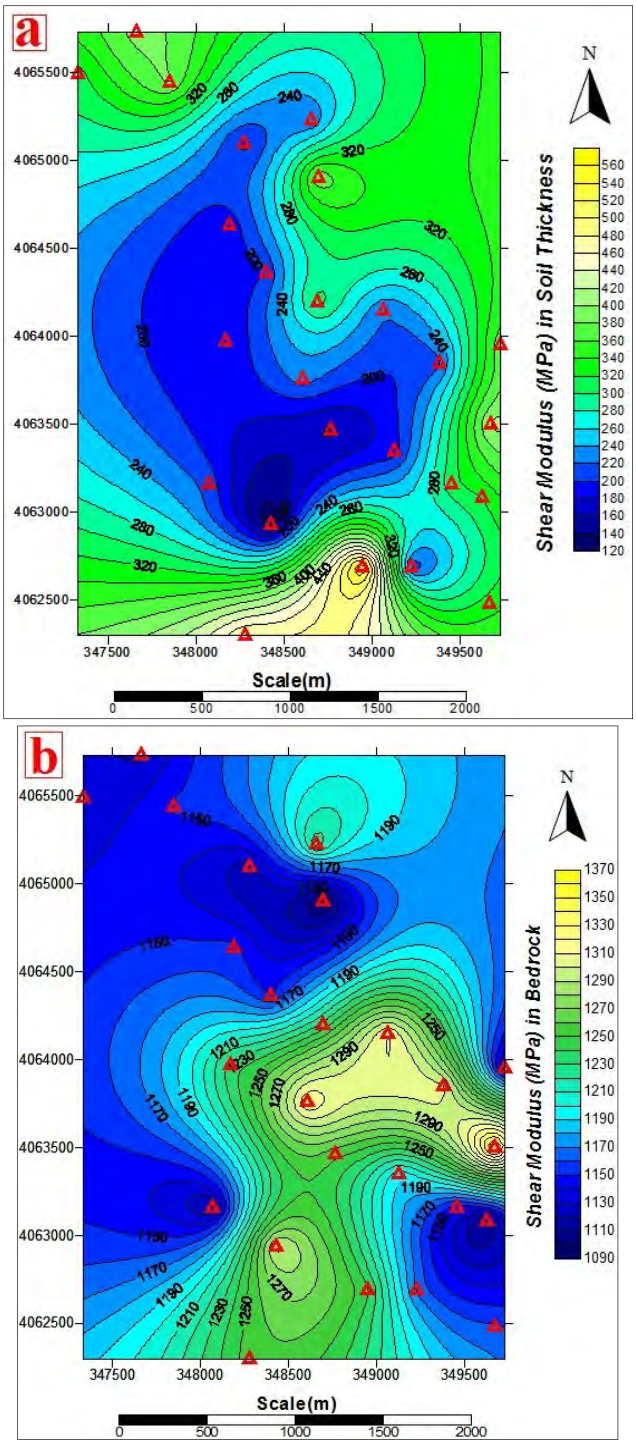

Fig. 12 Shear modulus (G) distribution contour map in the study area. (a) soil layer and (b) bedrock layer.

Table 3 Soil description with respect to Poisson's ratio ([12]).

Soil description parameter	Incompetent to slightly competent	Fairly to moderately competent	Competent materials	Very high competent materials
Poisson's ratio (ν)	0.41-0.49	0.35-0.27	0.25-0.16	0.12-0.03

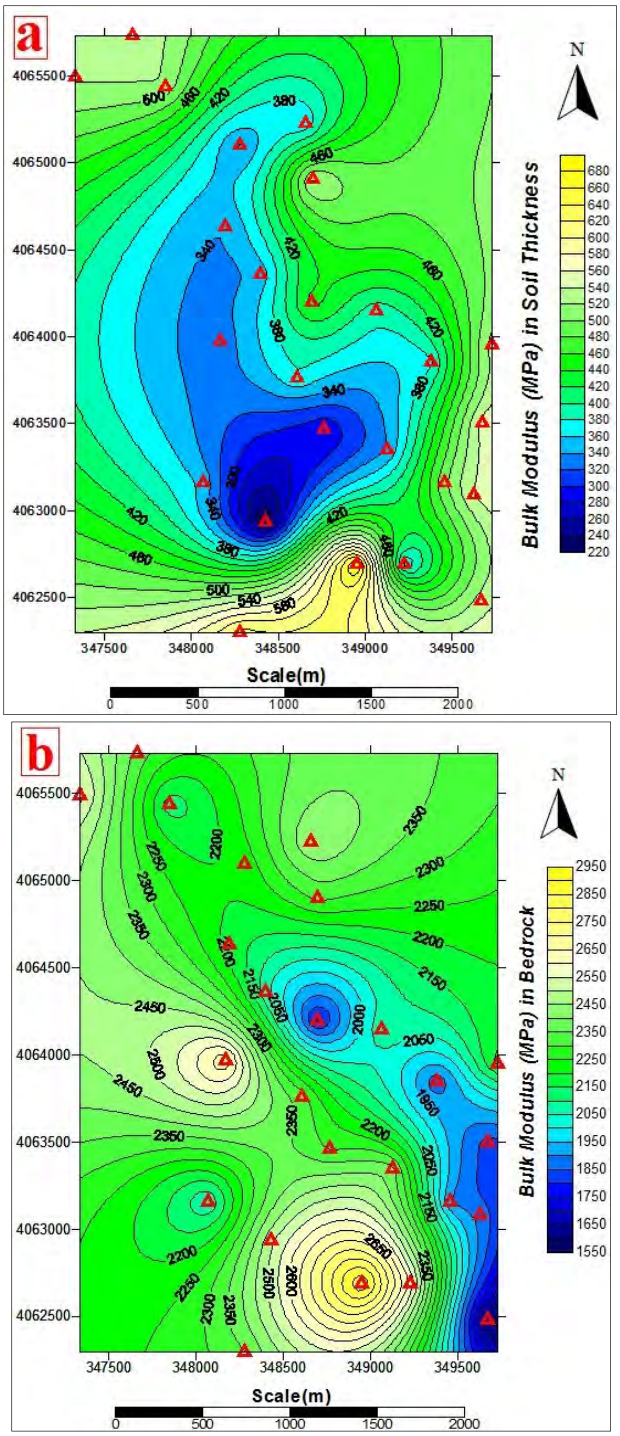

Fig. 13 Bulk modulus (K) distribution contour map in the study area. (a) soil layer and (b) bedrock layer.

Table 4 The ranges of seismic characteristics and elastic parameters in the second zone of the study area.

Parameter	Range
P-wave velocity	640-920 m/s
S-wave velocity	360-576 m/s
Amplification factor	1.26-1.65
Poisson's ratio	0.178-0.260
Young's modulus	500-1334 MPa
Shear modulus	200-566 MPa
Bulk modulus	340-690 MPa

6. Conclusion

The main objective of this study was to evaluate the geotechnical properties of soil deposits using seismic wave velocities measurements for power plants construction purposes. The resulted wave velocities information used to predict the seismic hazard level and dynamic behavior of near-surface structures. For achieving to this objective, a total numbers of 25 shallow P-wave seismic refraction profiles were acquired and then interpreted at the study area. For each profile, the average P-wave velocity of soil and bedrock layers were calculated by using the seismic refraction tomography (SRT) method and then the distribution maps of P-wave velocities were delineated. We then utilized the multi-channel analysis of surface wave (MASW) technique as a reliable, cost-effective and non-invasive method in order to obtain the S-wave velocities. By using the dispersion characteristics of recorded Rayleigh wave on the collected shot gathers and then the inversion technique, the S-wave velocity variation with depth was generated for each profile. In follow, distribution maps of S-wave velocities were constructed for the soil and bedrock layers by interpolating the resulted information. Seismic hazard parameters and dynamic soil properties at the site were evaluated and micro-zonation of the study area was carried out. The obtained results were used mainly to recommend the northern, eastern and southern regions of the study area as zones with more competent soil deposits and less hazard risk for any engineering purposes. The discussed geophysical methods in this study can be applied at any other sites where preserving the in-situ conditions and environmental factors at the time of testing are important.

7. References

[1] Alsaigh, N. H., Alheety, A. J. Seismic refraction tomography and MASW survey for geotechnical evaluation of soil for the teaching hospital project at Mosul University. Journal of Zankoy Sulaimani-Part A (JZS-A), 2014: 16 (1), 1-13.
[2] Anbazhagan, P., Sitharam, T. Site characterization and site response studies using shear wave velocity. Journal of Seismology and Earthquake Engineering, 2008: 10 (2), 53-67.
[3] Azwin, I. N., Saad, R. Nordina, M. Applying the seismic refraction tomography for site characterization. APCBEE Procedia, 2013: 5, 227-231.
[4] Bery, A. A. High resolution in seismic refraction tomography for environmental study. International Journal of Geosciences, 2013: 4, 792-796.
[5] Bery, A. A., Saad, R. Correlation of seismic P-wave velocities with engineering parameters (N value and rock quality) for tropical environmental study. International Journal of Geosciences, 2012: 3 (4), 749-757.
[6] Bery, A. A., Saad, R., Jinmin, M. Seismic refraction tomography for environmental study. 83rd Nationl Geosciences Conference. Geophysics Section. Malaysia. 2013.
[7] Boominathan, A. Seismic site characterization for nuclear structures and power plants. Geotechnical and Earthquake Hazards, 25 November 2004: 85 (10), 1388-1397.
[8] Building Seismic Safety Council. NEHRP recommended provisions for seismic regulations for new buildings and other structures, Part: Provisions, FEMA 450, Federal Emergency Management Agency, Washington, D.C. 2003.
[9] Dowrick, D. Earthquake risk reduction. John Wiley and Sons, New York. 2003.
[10] Gardner, G. H. F., Gardner, L. W., Gregory, A. R. Formation velocity and density; the diagnostic basics for stratigraphic traps. Geophysics, 1974: 39, 770-780.
[11] Joyner, W. B., Warrick, R. E., Fumal, T. E. The effect of quaternary alluvium on strong ground motion in the Coyote Lake, California, earthquake of 1979. Bull Seismol Soc Am, 1981: 71, 1333-49.
[12] Khalil, M. H., Hanafy, S. M. Engineering applications of seismic refraction method: A field example at WadiWardan, Northeast Gulf of Suez, Sinai, Egypt. Journal of Applied Geophysics, 2008: 65, 132-141.
[13] Luna, R., Jadi, Houda. Determination of Dynamic Soil Properties Using Geophysical Methods. Proceedings of the First International Conference on the Application of Geophysical and NDT Methodologies to Transportation Facilities and Infrastructure, St. Louis, MO, December 2000.
[14] Mahajan, A. K., Slob, S., Ranjan, R., Sporry, R., Ray, P. K. C., Westen, C. J, V. Seismic microzonation of Dehradun city using geophysical and geotechnical characteristics in the upper 30 m of soil column. Journal of Seismology, 2007: 11, 355–370.
[15] Mohamed, A. M. E., Abu El-Ata, A. S. A., Abdel Azim, F., Taha, M. A. Site-specific shear wave velocity investigation for geotechnical engineering applications using seismic refraction and 2D Multi-channel Analysis of Surface Waves. NRIAG Journal of Astronomy and Geophysics, 2013: 2, 88-101.
[16] Park, C. B., Miller, R. D., Xia, J., Ivanov, J. Multichannel analysis of surface waves (MASW)—active and passive methods. The Leading Edge, 2007: 26, 60-64.

[17] Penumadu, D., Park, C. B. Multichannel analysis of surface wave (MASW) method for geotechnical site characterization. Earthquake engineering and soil Dynamics, 2005: 158 (3), 1-10.
[18] Rao, K. S., Gupta, K. K., Rathod, G. W., Trivedi, S. S. Integration geophysical studies with engineering parameters for seismic microzonation. Indian Geotechnical Conference. 2009, Guntur, India.
[19] Satyam, D. N., Rao, K. S. Multichannel analysis of surface wave (MASW) testing for dynamic site characterization of Delhi region. Fifth International Conference on Recent Advances on Geotechnical Earthquake Engineering and Soil Dynamics and Symposium in Honor of Professor I. M. Idriss. 24-29 May 2010, San Diago, California.
[20] Sheehan, J. R., Doll, W. E., Mandell, A. An evaluation of methods and available software for seismic refraction tomography analysis. Journal of Environmental and Engineering Geophysics, 2005: 10 (1), 21-34.
[21] Sheriff, R. E., Geldart, L. P. Exploration seismology: 2nd Edition, Cambridge University Press, New York, USA, 1995.
[22] Sloan, S. D., Nolan, J. J., Broadfoot, S. W., Mckenna, J. R., Metheny, O. M. Using near-surface seismic refraction tomography and multichannel analysis of surface waves to detect shallow tunnels: A feasibility study. Journal of Applied Geophysics, 2013: 99, 60-65.
[23] Thitimakorn, T., Channoo, S. Shear wave velocity of soils and NEHRP site classification map of chiangrai city, northern Thailand. Electronic Journal of Geotechnical Engineering, 2012: 17, 2891- 2904.
[24] Thurber, C., Ritsema, J. Theory and Observations – Seismic Tomography and Inverse Methods. Treatise on Geophysics. 2007: 1, 323-360.
[25] Tian, G., Steeples, D.W., Xia, J., Miller, R.D. Multichannel analysis of surface wave method with the auto juggle. Soil Dynamics and Earthquake Engineering, 2003: 23, 243–247.
[26] Tokeshi, K., Harutoonian, P., Leo, C. J., Liyanapathirana, S. Use of surface waves for geotechnical engineering applications in Western Sydney. Advances in Geosciences, 2013: 35, 37-44.
[27] Xia, J., Miller, R.D., Park, C.B., Hunter, J.A., Harris, J.B. Comparing shear-wave velocity profiles from MASW with borehole measurements in unconsolidated sediments, Fraser River Delta, B.C. Journal of Environmental and Engineering Geophysics, 2000: 5(3), 1–13.
[28] Xia, J., Miller, R.D., Park, C.B., Hunter, J.A., Harris, J.B., Ivanov, J. Comparing shear-wave velocity profiles inverted from multichannel surface wave with borehole measurements. Soil Dynamics and Earthquake Engineering, 2002: 22, 181–190.